



Numerical simulation of Composition B high explosive charge desensitization in gap test assembly after loading by precursor wave

I. A. Balagansky¹ · A. A. Stepanov¹

Received: 15 October 2013 / Revised: 11 June 2015 / Accepted: 6 July 2015 / Published online: 18 July 2015
© Springer-Verlag Berlin Heidelberg 2015

Abstract Results of numerical research into the desensitization of high explosive charges in water gap test-based experimental assemblies are presented. The experimental data are discussed, and the analysis using ANSYS AUTO-DYN 14.5 is provided. The desensitization phenomenon is well reproduced in numerical simulation using the JWL EOS and the Lee–Tarver kinetic equation for modeling of the initiation of heterogeneous high explosives with as well as without shock front waves. The analysis of the wave processes occurring during the initiation of the acceptor HE charge has been carried out. Peculiarities of the wave processes in the water gap test assemblies, which can influence the results of sensitivity measurement, have been studied. In particular, it has been established that precursor waves in the walls of the gap test assemblies can influence the detonation transmission distance.

Keywords Water gap test · Numerical modeling · Desensitization · Composition B

1 Introduction

Every industrial or storage facility where high explosive materials are handled requires special measures for preventing sympathetic detonation in case of an explosion to reduce damage due to a chain reaction. This is why understanding the sympathetic detonation phenomenon is extremely important

for safety engineering. The gap test is one of the easiest and widely used methods for measuring shock sensitivity of high explosives. The results of impact sensitivity tests are often not reproducible, because factors in the explosion experiment that might affect the formation and growth of hot spots could strongly influence the measurements [1–3]. In particular, we have observed the phenomenon of desensitization of acceptor high explosive charges in gap test-based experimental assemblies that include water gaps and solid inert elements.

Papers [4–6] present the results of those experimental studies of the influence that inert inserts of different materials have on the detonation transmission and detonation failure distance in water. Donor and acceptor HE charges were made of cast Composition B (having density of 1.65 g/cm³) and shaped as cylindrical cartridges with diameter and height of 40 mm. On the rear end of the acceptor HE charge an identification steel specimen was mounted to detect the presence or absence of detonation. Inert inserts made of polytetrafluoroethylene (PTFE), copper, and silicon carbide shaped as 20 mm × 20 mm square prisms of varying heights Δ were placed between donor and acceptor charges without any clearance in the way of the initiating shock wave and with partial overlap of HE cross sections. The experimental assembly is shown in Fig. 1.

Distances for reliable detonation transmission, as well as failure distances for acceptor HE charge initiation through water have been measured without any inert insert and for inserts made of PTFE, copper, and silicon carbide of varying heights. In total, the authors have conducted 27 experiments. Experimental detonation transmission and detonation failure distances are presented in Table 1.

Thus, it has been demonstrated that explosive loading of an acceptor HE charge by a precursor wave through a copper or ceramic insert leads to its significant desensitization. With all other conditions being equal, the distance for copper has

Communicated by C. Needham and A. Higgins.

✉ I. A. Balagansky
balagansky@craft.nstu.ru

¹ Novosibirsk State Technical University, Novosibirsk 630073, Russia

been found to be 75 % and for silicon carbide only 60 % of the value for a PTFE insert.

It should be noted that for a silicon carbide insert the precursor wave is, in fact, a compression wave without a shock front, because it has been propagating in an elastic material [7]. The value of the Hugoniot elastic limit for silicon carbide is approximately 10 GPa.

The desensitization phenomena of heterogeneous high explosives under loading with a shock wave having a precursor of smaller amplitude are well-known [8–11]. The term “shock desensitization” is linked to a variety of phenomena in high explosives such as dead pressing, detonation extinction and the reduced response of explosives to multiple shocks. Thereby behavior of a high explosive as an inert substance can be achieved under considerably high pressures in the main shock wave. If the initial impulse has a precursor with amplitude insufficient for detonation initiation, pores in het-

erogeneous HE collapse, and charges do not detonate even if the pressure in the main shock wave considerably exceeds the level of reliable initiation.

Most researchers believe the desensitizing is the result of deactivating hot spots [8–10]. There are various theories as to the exact nature and role of hot spots in the initiation of high explosives. Perhaps there is general agreement that hot spots form from regions of low density that go to temperature much greater than average for the bulk material when shocked because, when they are compressed, more work is done locally than in the bulk full-density explosive [11]. They react to release energy and detonation products. A puzzling feature is that the hot spots, ignited by a relatively weak shock, do not continue to react and expand into the rest of the explosive. Explosive behind the thin layer is dead and does not react. A strong second shock sent behind the first into the dead explosive propagates as an inert shock. Not until the second shock overtakes the first shock and is moving into unshocked explosive does the initiation process start.

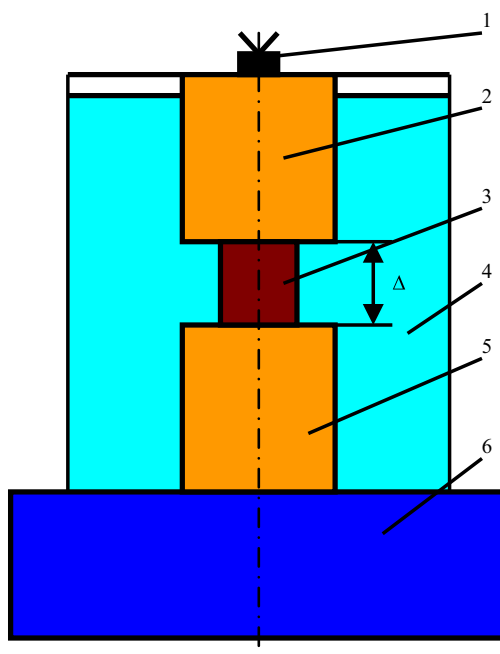


Fig. 1 Experimental assembly scheme: 1—electric detonator; 2—donor HE charge; 3—inert insert (shaped as a 20 × 20 mm square prism); 4—degassed water; 5—acceptor HE charge; 6—identification steel specimen

Table 1 Detonation transmission distances (experimental and calculated)

Inert insert material	Reliable detonation transmission distance (mm)		Failure distance (mm)	
	Experimental	Calculated	Experimental	Calculated
No inert insert	50	45	55	50
PTFE/PMMA	45	45	50	50
Copper	30	37	37	40
Silicon carbide	26	30	30	35

2 Numerical modeling

The goal of our work has been to study the wave processes in the water gap test-based experimental assemblies that lead to desensitization of acceptor Composition B charges after loading by a precursor wave passing through an inert element placed on the symmetry axis of the assembly. For this purpose, numerical simulation of the detonation transfer from donor to acceptor HE charges has been performed in the configuration most closely corresponding to the experimental conditions. Simulations were carried out using ANSYS AUTODYN 14.5 [12].

Simulation area configurations reproduced the experimental assemblies with one exception: instead of square 20 × 20 mm prisms used in the experiments, the simulated assembly included round rods with the diameter of 22 mm. Thus, we were able to use a 2D axisymmetric setup instead of 3D. Because of the axial symmetry, only half of the experimental assembly cross section has been modeled.

Numerical integration of the continuum mechanics equations together with defining parameters for materials and corresponding initial and boundary conditions has been per-

formed on a regular Eulerian mesh with a spatial resolution of 10 cells per mm. The detonation wave was initiated as a plane wave and propagated from the left to the right boundary of the Eulerian mesh. Boundary conditions on the left, right, and upper boundaries were defined in terms of AUTODYN as “Flow out.” The lower boundary was the symmetry axis.

The most difficult problem in numerical modeling is selecting the most appropriate model and the equation of state parameters for materials used in the simulation. EOS parameters for inert materials were selected from the standard library with the exception of silicon carbide, for which we have selected a model most closely corresponding to the experimental results of paper [7].

The Lee–Tarver ignition and growth model has been used to describe the behavior of the Composition B acceptor HE charge [13–16], etc. The model uses two Jones–Wilkins–Lee (JWL) equations of state, one for the unreacted explosive and another one for its reaction products, in the temperature-depended form

$$p = Ae^{-R_1 V} + Be^{-R_2 V} + \omega C_V T / V$$

where p is pressure, V is the relative volume, T is temperature, ω is the Grüneisen parameter, C_V is the average heat capacity, and A , B , R_1 , and R_2 are constants.

The chemical reaction rate law was first described in paper [13]. It was modified in paper [14]. The reaction rate law contains three terms to model the ignition of hot spots by shock compression, the slow growth of reaction from these isolated hot spots, and the rapid completion of reaction as the hot spots coalesce.

$$\begin{aligned} d\alpha/dt = & I(1-\alpha)^b(\rho/\rho_0 - 1 - a)^x + G_1(1-\alpha)^c\alpha^d p^y \\ & + G_2(1-\alpha)^e\alpha^g p^z \end{aligned}$$

where α is the fraction reacted (degree of HE decomposition), t is time, ρ is the current density, ρ_0 is the initial density, p is pressure, and I , G_1 , G_2 , a , b , c , d , e , g , x , y , and z are constants. The parameter a is the critical compression that is used to prohibit ignition until a certain degree of compression (or a certain input pressure) has been reached. This parameter provides the ability to calculate HE desensitization after precursor wave loading.

The best results [17] have been obtained using JWL EOS parameters for unreacted HE and detonation products for Composition B from the paper [18]. Values of kinetic constants corresponded to Composition B from the paper [19].

Table 2 shows equation of state parameters for silicon carbide, Table 3—for cast Composition B according to the terminology used in AUTODYN.

Table 1 shows the simulation versus experimental results for different materials (we have used PMMA instead of PTFE in the simulation).

Table 2 EOS parameters for silicon carbide

Reference density	3.10 g/cm ³
Grüneisen parameter	1.25
Parameter C_1	8.00 mm/μs
Parameter S_1	0.95
Strength	von Mises
Shear modulus	1.70 Mbar
Yield stress	0.065 Mbar
Failure	None

Table 3 EOS parameters for cast Composition B [18, 19]

Unreacted JWL	Product JWL
$A = 1479$ Mbar	$A = 5.308$ Mbar
$B = -0.05261$ Mbar	$B = 0.0783$ Mbar
$R_{1u} = 12$	$R_1 = 4.5$
$R_{2u} = 12$	$R_2 = 1.2$
$\omega_u = 0.912$	$\omega = 0.34$
$C_V = 2.487 \times 10^{-5}$ Mbar/K	$C_V = 1.0 \times 10^{-5}$ Mbar/K
$T_o = 298$ K	C–J energy/unit volume $E_{og} = 0.081$ Mbar
Shear modulus = 0.035 Mbar	C–J detonation velocity $U_D = 7.576$ mm/μs
Yield strength = 0.002 Mbar	C–J pressure $P_{CJ} = 0.265$ Mbar
$\rho_0 = 1.63$ g/cm ³	Reaction zone width $W_{reac} = 2.5$
Von Neumann spike rel vol. $c_0 = 0.7$	Max change in reaction ratio $\Delta\alpha_{max} = 0.1$
C–J energy/unit volume $E_{0,u} = -0.00504$ Mbar	
Reaction rates	
$a = 0.0367$	$x = 7.0$
$b = 0.667$	$y = 2.0$
$c = 0.667$	$z = 3.0$
$d = 0.333$	$F_{igmax} = 0.022$
$e = 0.222$	$F_{G1max} = 0.7$
$g = 1.0$	$F_{G2min} = 0.0$
$I = 4.0 \times 10^6$ μs ⁻¹	$G_1 = 140$ Mbar ⁻² μs ⁻¹
Maximum relative volume in tension = 1.1	$G_2 = 1000$ Mbar ⁻³ μs ⁻¹

Numerical modeling results demonstrate that the desensitization process in cast Composition B is reliably reproduced in simulation of precursor wave loading with or without a shock front using the chosen Lee–Tarver kinetic constants.

Initial configuration of the simulation area and detailed simulation results for a silicon carbide insert with $\Delta = 35$ mm are shown in Fig. 2 as material flow fields with pressure and degree of decomposition contours at different times. Color bars for the contour levels are given in Fig. 2 too. Initial configuration is shown in Fig. 2a.

Figure 2b shows the pressure contours and material flow fields at $t = 5.25 \mu\text{s}$, when the detonation front reaches the end of the donor HE charge. Pressure on the detonation wave front in the donor charge is 22.1 GPa. Material flow fields and decomposition contours at $t = 5.25 \mu\text{s}$ are shown in Fig. 2c. When this wave enters the silicon carbide rod, it produces a wave with front pressure of 28.1 GPa. At the same time, the initial pressure of the shock wave front in water is only 19.1 GPa. These two waves continue to propagate towards

the acceptor HE charge, with the wave in the rod moving ahead of the wave in water.

At $t = 8.50 \mu\text{s}$ the wave in the rod reaches the acceptor HE charge with an amplitude of 3.6 GPa and initiates a compression wave without a shock front in it with an amplitude of 2 GPa. The degree of decomposition of the acceptor charge equals zero (see Fig. 2d, e).

Figure 2f shows the material flow fields and pressure contours at $t = 14.25 \mu\text{s}$, when the initiating shock wave in

Fig. 2 Simulation of detonation transmission in a water gap test with a silicon carbide insert with height $\Delta = 35 \text{ mm}$. **a** Initial configuration; **b, d, f, h** material flow fields and pressure contours; **c, e, g, i** material flow fields and decomposition contours

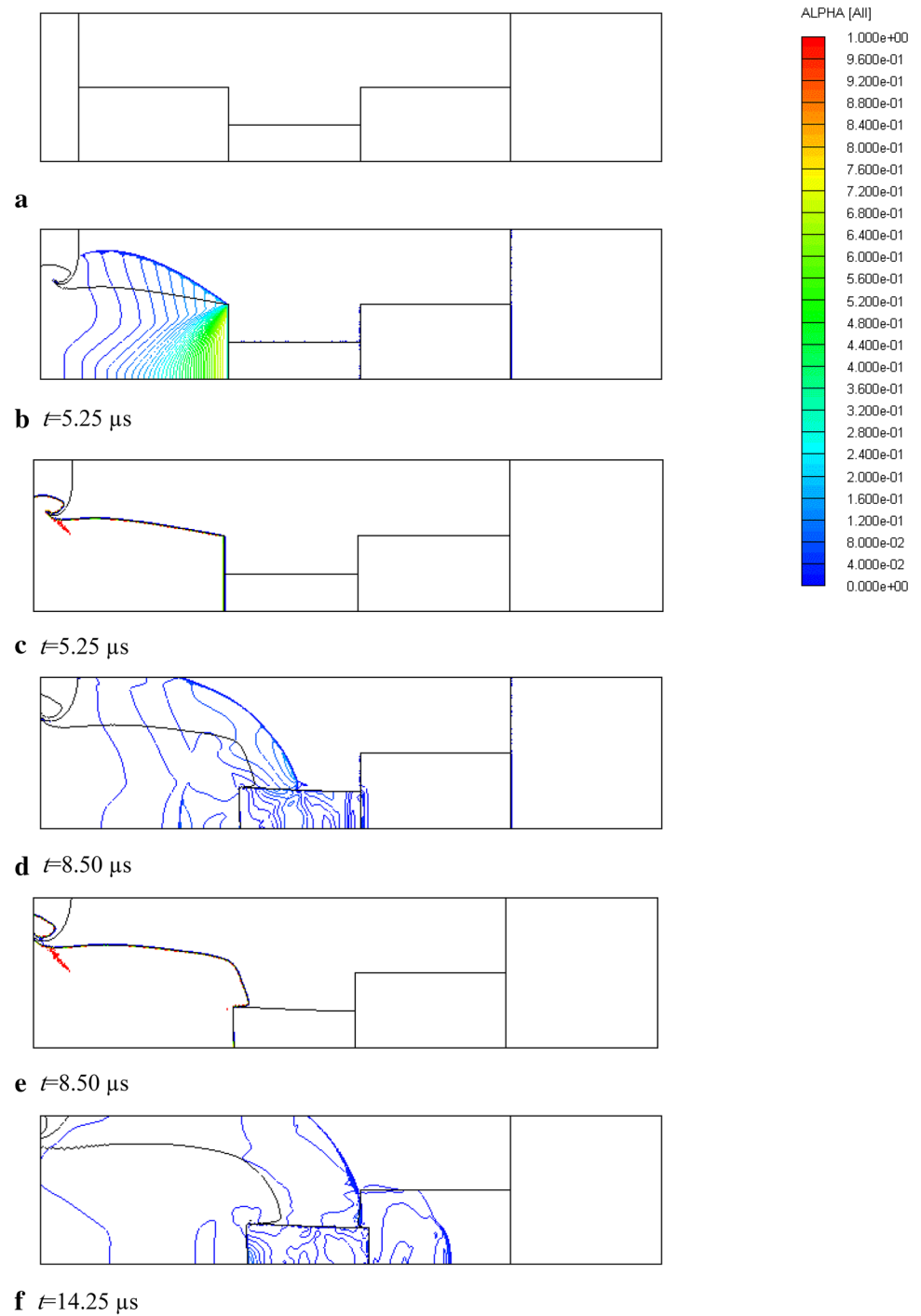
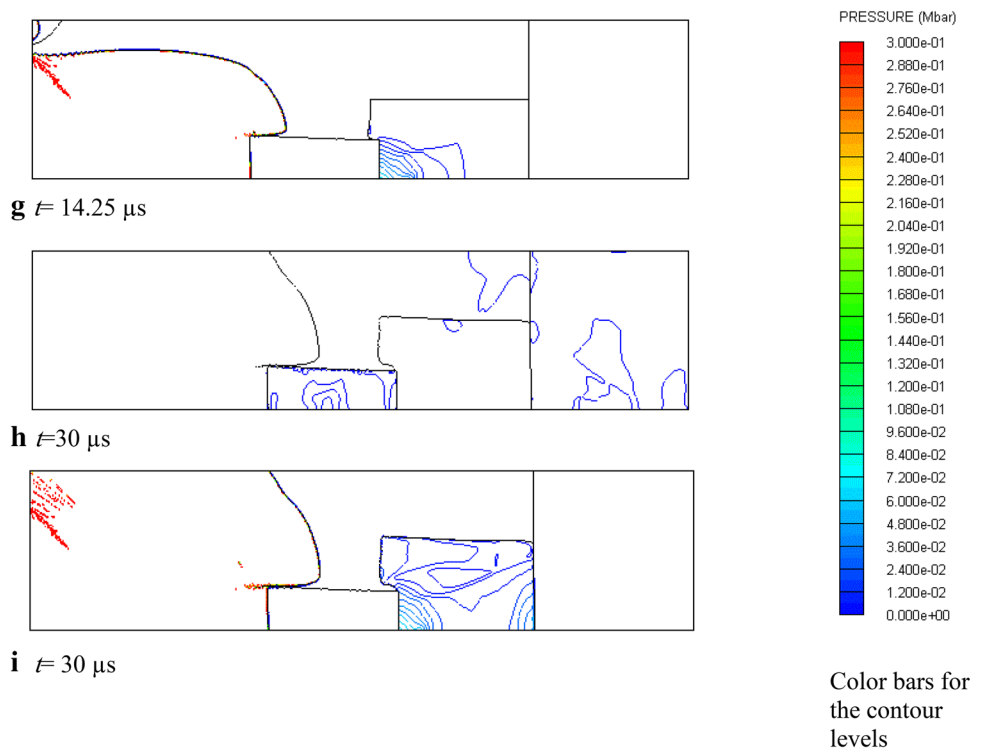


Fig. 2 continued

water reaches the acceptor HE charge and creates a wave in the peripheral area of the charge with an amplitude of 2 GPa. At the same time, the maximum pressure on the symmetry axis of the HE charge equals 4.6 GPa and the maximum degree of decomposition reaches 0.2 in the area near the end of the ceramic rod (see Fig. 2g).

Later the process continues to develop in a similar way. HE charge initiation on the symmetry axis does not develop. Initiation by the wave through water is not observed as well, because the wave propagates through the charge that has already been compressed by the precursor wave.

Figure 2h, i show the material flow fields and HE pressure and decomposition contours on the late stage of the process at $t = 30 \mu\text{s}$.

Figure 3 shows pressure and degree of decomposition profiles on the symmetry axis of acceptor HE charge at times of 14.25 and 30 μs .

The maximum pressure in the acceptor HE charge at $t = 30 \mu\text{s}$ equals 0.8 GPa. The maximum degree of decomposition is observed near the end of the ceramic rod and it has practically not changed since the moment $t = 14.25 \mu\text{s}$. Because of the reflection from the identification specimen, the process of initiation by the reflected wave is observed for some time and at $t = 30 \mu\text{s}$ the degree of decomposition reaches approximately 0.15.

Thus, it is shown that precursor waves in gap test assemblies can influence the detonation transmission distance due to desensitization of the acceptor HE charge. It is also shown

that the presence of the identification steel specimen can lead to erroneous results when using the gap test due to possible initiation of acceptor HE charge by the wave reflected from the specimen.

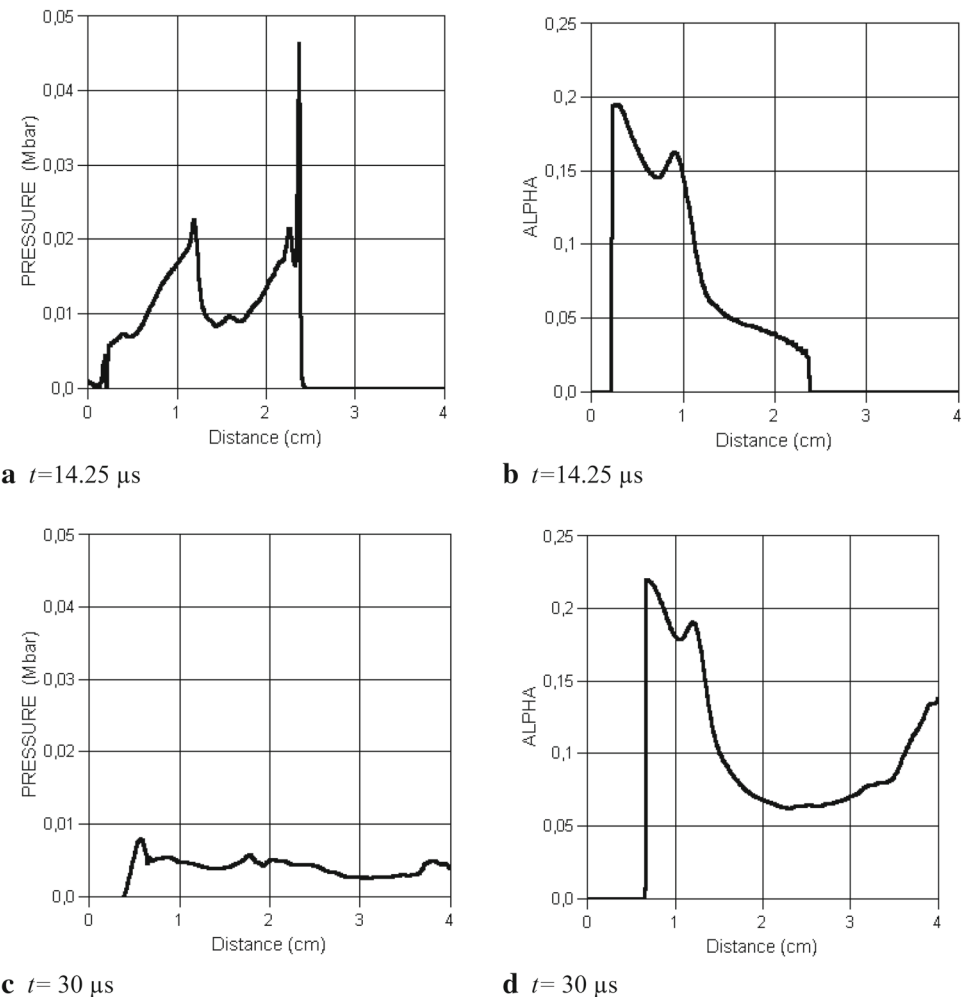
3 Conclusions

The results of numerical modeling of the desensitization of high explosive charges in water gap test-based experimental assemblies are presented. The desensitization phenomenon is well reproduced in numerical simulation using the Lee–Tarver kinetic equation for modeling of the initiation of heterogeneous high explosives with as well as without shock front waves.

Analysis of the wave processes occurring during the initiation of the acceptor HE charge has been performed. Peculiarities of the wave processes in the gap test assemblies that can influence the results of sensitivity measurements have been studied. In particular, it has been established that precursor waves in gap test assemblies can influence the detonation transmission distance. It is also shown that the presence of the identification steel specimen can lead to erroneous results when using the gap test due to possible initiation of acceptor HE charge by the wave reflected from the specimen.

Summarizing the foregoing, we would like to recommend when analyzing the gap test results to take into account the

Fig. 3 Pressure (**a, c**) and degree of decomposition (**b, d**) profiles on the symmetry axis of acceptor HE charge from $x_1 = 8.5 \text{ cm}$ to $x_2 = 12.5 \text{ cm}$ at different times



possibility of acceptor charge desensitization by precursor waves, and its possible initiation by the wave reflected from an identification specimen.

Acknowledgments This work was partially supported by the Russian Foundation for Basic Research (Projects Nos. 06-08-0138 and 14-08-00068).

References

1. Keshavarz, M.H., Motamedshariati, H., Pouretedal, H.R., Tehrani, M.K., Semnani, A.: Prediction of shock sensitivity of explosives based on small-scale gap test. *J. Hazard. Mater.* **145**, 109–112 (2007)
2. Lefrancois, A.S., Lee, R.S., Tarver, C.M.: Shock desensitization effect in the confined explosive component water gap test defined by the NATO standardization agreement (STANAG) 4363. *Propellants Explos. Pyrotech.* **32**, 244–250 (2007)
3. Kubota, S., Liu, Z., Otsuki, M., Nakayama, Y., Ogata, Yu., Yoshida, M.: A numerical study of sympathetic detonation in gap test. *Mater. Sci. Forum* **465–466**, 163–168 (2004)
4. Balagansky, I.A., Matrosov, A.D., Stadnichenko, I.A., Samsonov, A.V., Glumov, A.I.: Behavior of condensed heterogeneous high explosive under shock wave loading through water after preloading with advanced wave. *Rep. Russ. Higher Educ. Acad. Sci.* **2**, 76–83 (2007)
5. Balagansky, I.A., Matrosov, A.D., Stadnichenko, I.A., Glumov, A.I., Samsonov, A.V.: Influence of inert copper and silicon carbide inserts on process of detonation transmission through water. *Mater. Sci. Forum* **566**, 207–212 (2008)
6. Balagansky, I.A., Matrosov, A.D., Stadnichenko, I.A., Glumov, A.I., Samsonov, A.V.: Desensitization of heterogeneous high explosives under initiation through high modulus elastic elements. *Int. J. Mod. Phys. B* **22**, 1305–1310 (2008)
7. Balagansky, I.A., Balagansky, A.I., Razorenov, S.V., Utkin, A.V.: Evolution of shock waves in silicon carbide rods. In: Furnish, M.D., Elert, M., Russell, T.P., White, C.T. (eds.) *Proceedings of the 14th APS Topical Conference on Shock Compression of Condensed Matter*, (AIP Conference Proceedings), vol. 845, pp. 835–838. (2006)
8. Jacobs, S.J.: Non-steady detonation. In: *Proceedings of 3rd Symposium on Detonation*, pp. 784–812. (1960)
9. Campbell, A.W., Davis, W.C., Ramsay, J.B., Travis, J.R.: Shock initiation of solid explosives. *Phys. Fluids* **4**, 511–521 (1961)

10. Campbell, A.W., Travis, J.R.: The shock desensitization of PBX-9404 and Composition B-3. In: Proceedings of 8th Symposium (International) on Detonation, pp.1057–1068. (1985)
11. Davis, W.C.: Shock desensitizing of solid explosive. In: Proceedings of 14th International Detonation Symposium, pp. 1058–1064. (2010)
12. AUTODYN, Explicit Software for Nonlinear Dynamics, Theory Manual, (Century Dynamics) (2005)
13. Lee, E.L., Tarver, C.M.: Phenomenological model of shock initiation in heterogeneous explosives. *Phys. Fluids* **23**, 2362–2372 (1980)
14. Tarver, C.M., Hallquist, J.O., Erickson, L.M.: Modeling short pulse duration shock initiation of solid explosives. In: Proceedings of 8th Symposium (International) on Detonation, pp. 951–961. (1985)
15. Tarver, C.M., Cook, T.M., Urtiew, P.A., Tao, W.C.: Multiple shock initiation of LX-17. In: Proceedings of 10th International Detonation Symposium, pp. 696–703. (1993)
16. Kury, J.W., Don Breithaupt, R., Tarver, C.M.: Detonation waves in trinitrotoluene. *Shock Waves* **9**, 227–237 (1999)
17. Balagansky, I.A., Hokamoto, K., Manikandan, P., Matrosov, A.D., Stadnichenko, I.A., Miyoshi, H., Bataev, I.A., Bataev, A.A.: Mach stem formation in explosion systems, which include high modulus elastic elements. *J. Appl. Phys* **110**, 123516 (2011)
18. Murphy, M.J., Lee, E.L., Weston, A.M., Williams, A.E.: Modeling shock initiation in Composition B. In: Proceedings of 10th International Detonation Symposium, pp. 963–970. (1993)
19. Urtiew, P.A., Vandersall, K.S., Tarver, C.M., Garcia, F., Forbes, J.W.: Shock initiation experiments and modeling of Composition B and C-4. In: Proceedings of 13th International Detonation Symposium, pp. 929–939. (2007)